MULTISCIA JOURNALS PUBLISHERS

FRONTIERS IN MATERIAL SCIENCE AND NANOTECHNOLOGY

ISSN: (3065- 4114)

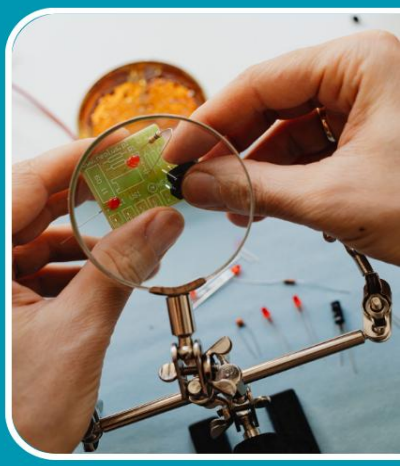

editor.fmsnt@gmail.com

https://multisciajournals.com/journals/index.php/fmsnt

Frontiers in Material Science and Nanotechnology
Volume1, Issue1, 2025

Impact on Living Things Penetration of the Tetra-Branched Anti-TNF-Peptide Dependent on the Coating Ratio Transtympanic Injection of Gamma-Maghemite Nanoparticles Stabilized by Conjugated Cerium3/4+ and Visualized by Magnetic Resonance Imaging (MRI) into the Inner Ear of Rats

Kettunen UI[1], Lsellouche[2] ,Pyykköhj I[3]

[1]Department of **Material Science and Nanotechnology**

Article Info

Received: 30-01-2025 ***Revised:07-03-2025*** ***Accepted:17-03-2025*** ***Published:28-03-2025***

Abstract

Goal: After a transtympanic injection, determine the distribution of TBATP in the inner ear and assess their biological effectiveness. Approach: The TBATP was produced by means of the conventional Fmoc solid phase synthesis. It was in human umbilical vein endothelial cells (HUVECs) that a model of TNF-α-induced apoptosis was developed. The CAN-γ-Fe2O3 NPs were covalently linked to the peptides. The middle ear cavity of rats was injected with a suspension of nanoparticles. A 7.0 T MRI scanner, in conjunction with Prussian blue staining, was used to determine the distribution of CAN-γ-Fe2O3 NPs in the inner ear. Findings: The inhibitory impact on HUVECs caused by TNF-α was almost entirely mitigated by TBATP, in contrast to the linear one, which only mitigated half of the effect. At 3 hours and 2 days after administration to the middle ear, CAN-γ-Fe2O3 NPs conjugated to TBATP at a peptide weight ratio of 10% (but not 50%) effectively reached the inner ear, with the effect being most noticeable at 2 days.

In conclusion, the tetra-branched anti-TNF-α peptide (TBATP) can reduce the inhibitory effect of TNF-α on human umbilical vein endothelial cells (HUVECs). It can be seen using magnetic resonance imaging (MRI) after attaching to super-paramagnetic ceric ammonium nitrate cation-doped maghemite nanoparticles that are formed from the doping oxidation of starting magnetite nanoparticles (CAN-γ-Fe2O3 NPs). Inner ear, magnetic resonance imaging, peptides, functional maghemite nanoparticles, biological barrier

Introduction

Evidence suggests that tumor necrosis factor-α (TNF-α) cascades contribute to the deterioration of hearing in several pathologies, including noise-induced, abrupt sensorineural, age-related, and neonatal hyperbilirubinaemia-induced brain toxicity [1-6]. In cases of noise-induced hearing loss, it has been shown that using an antibody that blocks tumor necrosis factor α may enhance auditory function. systemic inflammatory disease of the auditory nerve [7-9]. Nevertheless, the therapeutic target cannot be reached by antibodies that target TNF-α due to their too high molecular weight. Antibodies are bulky and difficult to work with, but peptides are more manageable in size, storage stability, and flexibility. In order to mimic the structure of an antibody, scientists created a new tetra-branched anti-TNF-α peptide that could prevent the binding of human TNF-α to its receptors, after selecting it from a phage library [10]. Creating comparable treatments for inner ear disorders is therapeutically relevant.

Current clinical practice employs intratympanic delivery of medications as a method with benefits such as minimizing administration dose and preventing systemic side effects. A greater amount of gadolinium chelate was able to pass into the perimodiolar lymph and lateral wall of the mouse cochlea through intratympanic delivery compared to intravenous injection, according to in vivo MRI studies. This difference may be due to the potential porous structures of the medial wall of the scala tympani and the spiral ligament extracellular space [11]. Drug distribution to the modiolus and lateral wall of the cochlea may be facilitated via the intratympanic pathway if drugs could be efficiently passed into these locations. One dependable way to monitor the dynamics of the administered drugs is to in vivo track their dispersion in the targeted organ. We have recently made public the creation of super-paramagnetic maghemite nanoparticles (NPs) that are both hydrophilic and anti-aggregative. These NPs were made using ceric ammonium nitrate (CAN) to oxidize starting magnetite (Fe3O4) NPs. The result was aqueous suspensions/ferrofluids that were exceptionally stable, thanks to a novel ultrasound-mediated doping process that used lanthanide Ce3/4+ cations on the surface of the Fe3O4 NPs [12]. We have also shown that the new CAN-γ-Fe2O3 NPs are an effective T2 MRI contrast agent that can penetrate both oval and circular windows. This suggests that they might be useful in molecular

imaging of the inner ear [13]. The current research set out to learn how, after being conjugated with MRI-traceable nanoparticles, medicines may be developed for use in inner ear treatment and diagnostics, and how they would traverse the round and oval windows. A prior research was used as a basis for the development of tetra-branched anti-TNF-α peptides, with some alterations [10]. In cell cultures, the peptides' biological effects in blocking cellular damage produced by TNF-α were examined. The in vivo magnetic resonance imaging (MRI) distributions in the inner ear of rats after middle ear injection were examined by analyzing the particular peptides conjugated to CAN-γ-Fe2O3 nanoparticles at different ratios.

Materials and Methods

Synthesization and Characterization of Tetra-Branched Anti-TNF-α Peptide

The sequences of effective peptide were HIHDDLLRYYGW, and that of scramble peptide were HDYLHRILGYDW. The selected peptides were synthesized in a tetrameric form (Figure 1) through standard Fmoc solid phase synthesis, building the tetramer on a three-lysine core and polyethylene glycol tail [10]. The synthesis was performed on a Sophas P1 S Solid Phase Peptide Synthesizer (Zinsser Analytic GmbH, Frankfurt, Germany) using [Fmoc-Lys(Fmoc)]2-Lys-βAla-2Cl Resin (0.15 mmol/g) (Shanghai Top-Peptide Biotechnology Co. Ltd., Shanghai, China), Fmoc-amino acids (0.5 mol/L), 2-(1H-benzotriazol-1-yl)-1,1,3,3-tetramethyluronium hexafluorophosphate (0.25 mol/L), *N,N*-Diisopropylethylamine (0.3 mol/L) (GL Biochem Co. Ltd., Shanghai, China) through rinse, deprotection, and ligase circles.

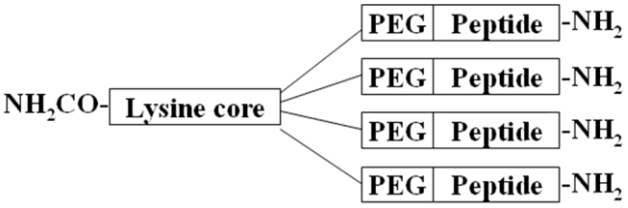

Figure 1: Schema of the tetra-branched peptides

For characterization, the peptide-resin complexes were pyrolyzed at room temperature for 3 h in the following solutions, trifluoroacetic acid: 3-hydroxytoluene: thioanisole: H_2O: ethane-1,2-dithiol=82.5: 5: 5: 5: 2.5. After removing the resin through filtration, the peptides were sedimentated using ice ether, centrifugated at 2362.5 g (4 °C) for 7 times, and then lyophilized. The samples (1 mg/mL, 50 μl) were run on an Agilent HPLC 1100 equipped with a column of Agilent 300SB-C18 4.6*250mm. The mobile phase A was composed of 0.1% trifluoroacetic acid in H_2O, and mobile phase B was composed of 0.1% trifluoroacetic acid in acetonitrile. The elution gradient was created by mixing A and B at various ratio at different time points. B: A=1/4, 2/3, 3/2, 9/1, and 1/4 at 0, 15, 25, 30, and 35 min. 5μm (Agilent Technologies, California, USA) at an elution speed of 1.0 mL/min and temperature of 40 °C.

Impact of Tetra-Branched Anti-TNF-α Peptide on Cellular Toxicity Induced by TNF-α

The first step was to use tumor necrosis factor α (TNF-α) to create a biological model of cell death in HUVECs (Supplementary material 1). The effect of tetra-branched anti-TNF-α peptide on cellular toxicity caused by TNF-α was examined after optimizing with different doses of TNF-α to construct the cell model of apoptosis in HUVECs. As previously stated, HUVECs were cultured. After the cells had grown into a confluent monolayer after 24 hours, 100 μL of the subsequent

Each well was treated with solutions six times. A. Negative control without any treatment; B. TNF-α (40 ng/mL)+tetra-branched anti-TNF-α peptide (0 μg/ mL); C. TNF-α (40 ng/mL)+tetra-branched anti-TNF-α peptide (25 μg/ mL); D. TNF-α (40 ng/ mL)+tetra-branched anti-TNF-α peptide (50 μg/ mL); E. TNF-α (40 ng/mL)+tetra-branched anti-TNF-α peptide (100 μg/ mL); F. TNF-α (40 ng/mL)+tetra-branched anti-TNF-α peptide (200 μg/ mL); G. TNF-α (40 ng/mL)+tetra-branched anti-TNF-α peptide (400 μg/ mL). Following the procedures outlined earlier, the MTT test and baseline reference were conducted. We evaluated the intervention effect of tetra-branched anti-TNF-α peptide with that of tetra-branched scrambled peptides, linear specific anti-TNF-α peptide, and linear scrambled peptides after optimizing optimum doses for suppressing apoptosis in HUVECs. The aforementioned methods were used to produce HUVECs. Once the cells had grown to a confluent monolayer after 24 hours of propagation, 100 μL of each solution was applied to each well six times. A. A control group that does not receive any treatment; B. TNF-α at a concentration of 40 ng/mL; C. TNF-α at a concentration of 40 ng/mL plus tetra-branched anti-TNF-α peptide at 200 μg/mL; D. TNF-α at a concentration of 40 ng/mL plus tetra-branched scrambled peptides at 200 μg/mL; E. A concentration of 40 ng/mL plus linear anti-TNF-α peptide at 800 μg/mL; F. A concentration of 40 ng/mL plus linear scrambled peptides at 800 μg/mL. Following the procedures outlined in Supplementary material 1, the baseline reference MTT tests were conducted.

.

Preparation and Characterization of Tetra-Branched anti-TNF-α-Peptide-Conjugated CAN-γ-Fe_2O_3 NPs

All the specific chemicals and reagents (analytical grade and/or highest purity level) used in this study, i.e., $FeCl_3$•$6H_2O$, $FeCl_2$•$4H_2O$, NH_4OH (ACS reagent, 28-30%), ceric ammonium nitrate (CAN, $CeIV(NH_4)_2(NO_3)_6$) have been purchased from Sigma-Aldrich (Israel) and have been used without any further purification. Starting neat neutral magnetite (Fe_3O_4) nanoparticles (Fe_3O_4 NPs, basic Massart hydrolytic method) were prepared as nanocarrier (Supplementary material 2).

Experimental Procedure for Nanocarrier Fabrication with Tetra-Branched Anti-TNF-α-Peptide Covalent Attachment to CAN-γ-Fe_2O_3 NPs

Corresponding CAN-γ-Fe_2O_3 NPs aqueous suspension (1 mL, Fe=1.96 mg/mL –ICP-AES measurement) was diluted to 25.0 mL using milliQ-purified H_2O. Then, 0.196 mg and 0.98 mg of tetra-branched anti-TNF-α peptide (peptide/Fe Wt ratio: 10% and 50% respectively) were added to the NP suspension as an aqueous solution and the medium was shaken overnight at 15 °C (orbital shaker). At completion of peptide contacting/NP surface decoration, resulting tetra-branched anti-TNF-α $peptide_{10\%}$ - CAN-γ-Fe_2O_3 NPs and tetra-branched anti-TNF-α $peptide_{50\%}$ -CAN-γ-Fe_2O_3 were washed 3 times (3 x 10 mL ddH_2O) using an Amicon® Ultra-15 centrifugal filter device (100K) operated at 4,000 rpm (5 min) to afford cleaned tetra-branched anti-TNF-α $peptide_{10\%}$ -CAN-γ-Fe_2O_3 and tetra-branched anti-TNF-α $peptide_{50\%}$ -CAN-γ-Fe_2O_3 NPs. Covalent contact of tetra-branched anti-TNF-α peptide (10% and 50% wt ratio) with CAN-γ-Fe_2O_3 NPs procedure was performed as discussed above.

Middle Ear Administration of Tetra-Branched Anti-TNF-α-Peptide-Conjugated CAN–γ-Fe_2O_3 NPs and MRI of Rat Inner Ear

Four male Sprague Dawley rats (8 ears), weighing between 300 and 350 grams, were maintained in the animal laboratory of A.I. Virtanen Institute for Molecular Sciences, University of Eastern Finland. The animals were randomly assigned into 2 groups (NP10, NP-50) (Table 1). The left ear was utilized for the delivery, and the right side was used as a negative control (NC group in Table 1). All the animal experiments have been approved by the Ethical Committee of University of Tampere (permission: ESAVI/3033/04.10.03/2011). Animal care and experimental procedures were conducted in accordance with European legislation. Throughout the experiments, the animals were anesthetized with a 5% isoflurane–oxygen mixture (flow-rate 1.0 L/min) for induction and a 2% isoflurane–oxygen mixture for maintenance *via* a facemask. Intramuscular injection of enrofloxacin (Baytril®vet, Orion, Turku, Finland) at a dose of 10 mg/kg was applied before the intratympanic administration of NPs to prevent potential infection. The animal's eyes were protected with Viscotears® (Novartis Healthcare A/S, Copenhagen, Denmark). The peptide-conjugated CAN-γ-Fe2O3 NPs were administered to the middle ear cavity with an injection tube by touching the surface of the tympanic medial wall according to a previously reported procedure [13,14]. A total volume of 10 µL of undiluted CAN-γ-Fe2O3 NP suspension was injected onto the medial wall of the middle ear cavity. The animals remained in the lateral position with the injected ear upward for 15 min before MRI study. After the last MRI measurement, the animals were decapitated for Prussian blue staining for iron in the tissue (Supplementary material 3) (Table 1).

Measurements	Number of ears		
	NP-10	NP-50	NC
MRI	2	2	4*
Prussian blue Staining	2	2	4*

MRI studies were performed at the time points of 3 h, 1 d, and 2 w post-middle ear administrations. **NC**: negative control; **NP-10**: CAN-γ-Fe_2O_3 NPs were conjugated to tetra-branched anti-TNF-α- peptide at 10% peptide ratio; **NP-50:** CAN-γ-Fe_2O_3 NPs were conjugated to tetra-branched anti- TNF-α peptide at 50% peptide ratio. *The right ear of each animal was used as **NC** in all studies. **Table 1:** Assignments of rat ears in MRI measurements and histology post-middle ear administration of tetra-branched anti-TNF-α-peptide-conjugated CAN-γ-Fe_2O_3 NPs

Statistics

In cell culture study, inhibition ratios on cell viability by different treatments were compared using one-way analysis of variance. Values of $p<0.05$ were accepted as statistically significant.

Results

Characterization of Tetra-Branched Anti-TNF-α Peptide and the Inhibiting Effect on Apoptosis of HUVECs Induced By TNF-α

High performance liquid chromatography shown a distinct peak for both the tetra-branched anti-TNF-α and scramble peptides, confirming their purity (Figure 2). Based on past experience, the additional abrupt peaks might be linked to partial fracture of the side chain's protective group. After 24 hours of incubation, a concentration-dependent response was seen in the cell viability of HUVECs treated with TNF-α, demonstrating the effective establishment of a cell model of apoptosis. The next tests were conducted with TNF-α protein at 40 ng/mL since this dose triggered apoptosis in 30.1% of the cells on average (Figure 3A). In a dosage-dependent response, the inhibitory impact on HUVECs generated by TNF-α was reduced by tetra-branched anti-TNF-α peptide. In the subsequent investigation, additional peptides were compared to 200 μg/mL of the peptides, which showed a maximum effect of 69.2% (Figure 3B). Figure 3C shows that the tetra-branched anti-TNF-α peptide had a much higher inhibitory impact on HUVECs produced by TNF-α, while the linear anti-TNF-α peptide had a significantly lower inhibitory effect.

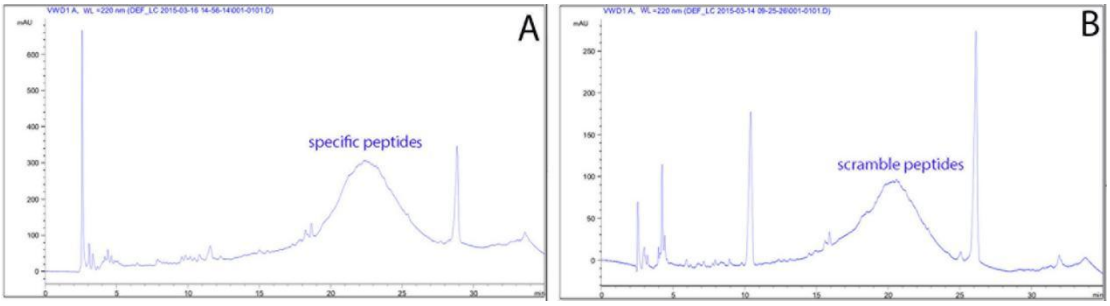

Figure 2: High performance liquid chromatography of tetra-branched anti-TNF-α peptide. The unique peak corresponds to either the specific peptides (A) or scramble peptides (B). The other sharp peaks might be associated with incomplete cracking of the protecting group for the side chain

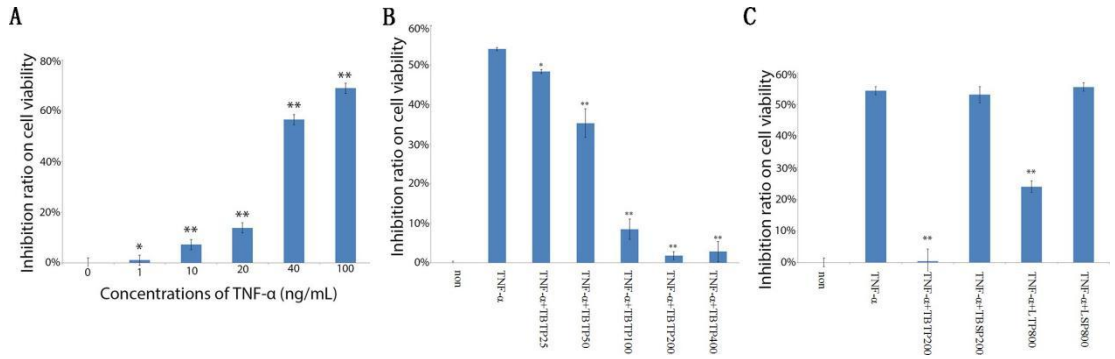

Figure 3: TNF-α-induced human umbilical vein endothelial cell death and intervention effect of anti-TNF peptides. **A.** Dose response of inhibition on viability of human umbilical vein endothelial cells induced by TNF-α. **B.** Dose response of tetra-branched TNF peptides on inhibitory effect of TNF-α in human umbilical vein endothelial cells. **C.** Impacts of various tetra-branched peptides on inhibitory effect of TNF-α in human umbilical vein endothelial cells. MTT assay was applied to evaluate the inhibitory effect. *p<0.05; **p<0.01 (one-way analysis of variance comparing to group 0 in A or group TNF-α in **B** and **C**). TNF-α+LSP800: cells were treated with TNF-α (40 ng/mL) plus linear scramble peptides (800 μg/mL); TNF-α+LTP800: TNF-α (40 ng/mL) plus linear anti-TNF-α peptide (800 μg/mL); TNF-α+TBSP200: TNF-α (40 ng/mL)+tetra-branched scramble peptide (200 μg/ mL); TNF-α+TBTP25: TNF-α (40 ng/mL)+tetra-branched anti-TNF-α peptide (25 μg/ mL); TNF-α+TBTP50: TNF-α (40 ng/mL)+tetra-branched anti-TNF-α peptide (50 μg/ mL); TNF-α+TBTP100: TNF-α (40 ng/ mL)+tetra-branched anti-TNF-α peptide (100 μg/ mL); TNF-α+TBTP200: TNF-α (40 ng/mL)+tetra-branched anti-TNF-α peptide (200 μg/ mL); TNF-α+TBTP400: TNF-α (40 ng/mL)+tetra-branched anti-TNF-α peptide (400 μg/ mL)

Characterization of Tetra-Branched Anti-TNF-α-Peptide-Conjugated CAN-γ-Fe_2O_3 NPs

The neat CAN-γ-Fe_2O_3 NPs has an average DLS size of 45.8 nm, and every 10% peptides conjugated to the NPs increased around 5 nm to the DLS diameter of the NPs. The neat CAN-γ-Fe_2O_3 NPs has an average ζ potential of +48 mV, and every 10% peptides conjugated to the NPs reduced approximally 5 mV of ζ potential (Table 2, Figure 4).

NPs	DLS (nm)	ζ potential (mV)
CAN-γ-Fe_2O_3	45.8	+48.0
0310A10% -CAN-γ-Fe_2O_3	49.68	+43.8
0310A50% -CAN-γ-Fe_2O_3	70.63	+24.8

CAN-γ-Fe_2O_3: neat NPs without peptide conjugation; $0310A_{10\%}$ -CAN-γ-Fe_2O_3: covalent contact of tetra-branched anti-TNF-α peptide at 10%wt ratio with CAN-γ-Fe_2O_3 NPs; $0310A_{50\%}$ -CAN-γ-Fe_2O_3: covalent contact of tetra-branched anti-TNF-α peptide at 50%wt ratio with CAN-γ-Fe_2O_3 NPs

Table 2: DLS and ζ potential results for neat CAN-γ-Fe_2O_3 NPs ($Ce^{3/4+}$)-doped maghemite (γ-Fe_2O_3) and peptide-conjugated NPs

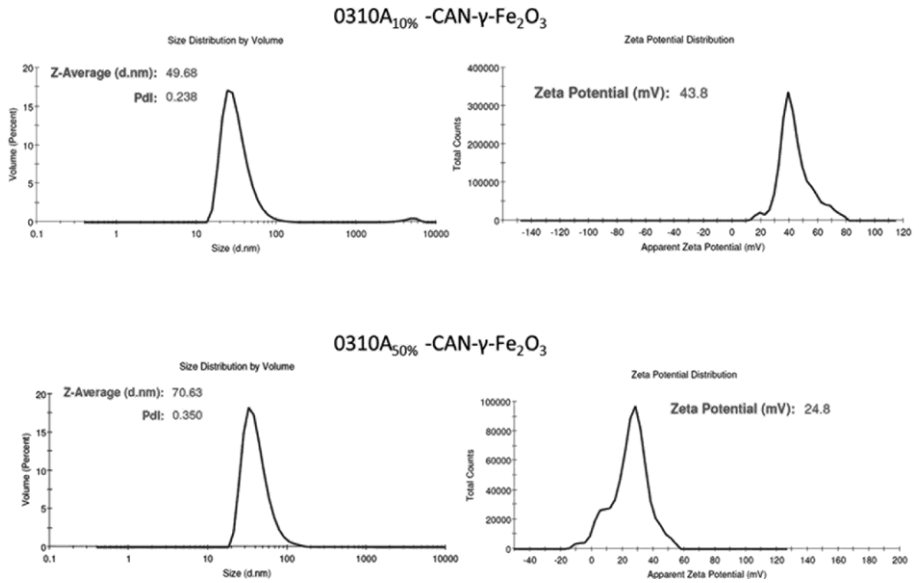

Figure 4: DLS and ζ potential results for neat CAN-γ-Fe_2O_3 NPs ($Ce^{3/4+}$)-doped maghemite (γ-Fe_2O_3 and peptide-conjugated NPs. $0310A_{10\%}$ -CAN-γ-Fe_2O_3: covalent contact of tetra-branched anti-TNF-α peptide at 10%wt ratio with CAN-γ-Fe_2O_3 NPs; $0310A_{50\%}$ -CAN-γ-Fe_2O_3: covalent contact of tetra-branched anti-TNF-α peptide at 50% wt ratio with CAN-γ-Fe_2O_3 NPs

Dynamic Distribution of Tetra-Branched Anti-TNF-Peptide-Conjugated CAN-γ-Fe_2O_3 NPs in Rat Inner Ear Shown by MRI

Significant morphological changes were detected in rat inner ear at 3 h through 2 w post-middle ear administrations of tetra-branched anti-TNF-α-peptide-conjugated CAN-γ-Fe_2O_3 NPs at 10% peptide ratio, which demonstrated that area of the ipsilateral cochlea basal turn, vestibule including the ampulla of semicircular canals shrinked in comparison to the contralateral ear (Figure 5). The changes were most pronounced at 2 w after administration, with typical wiping out of the perilymphatic spaces in the basal turn and hook region of the cochlea, and vestibule (Figure 6). This phenomenon was verified by injection of superparamagnetic iron oxide nanoparticles hierarchically coated with oleic acid and Pluronic® F127 copolymers into the scala tympani of rats. The

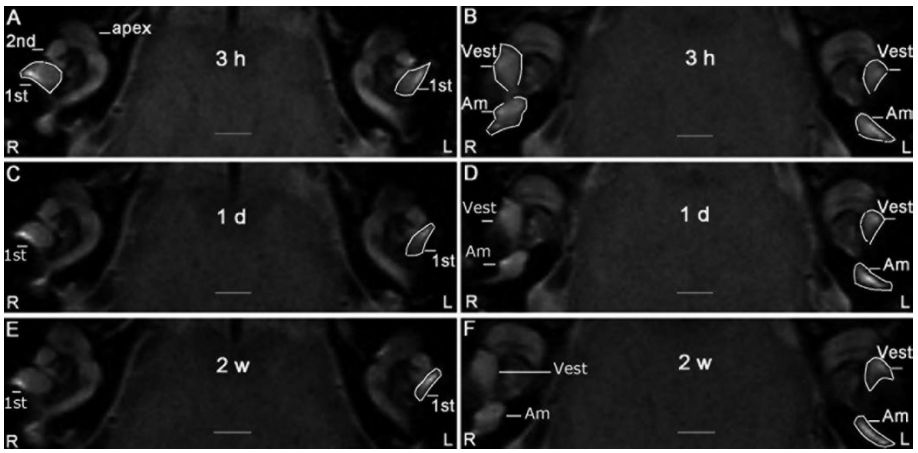

Figure 5: Efficient rat inner ear entry of tetra-branched anti-TNF-α-peptide-conjugated CAN-γ-Fe_2O_3 NPs at 10% peptide ratio shown by MRI. The bright area of inner ear fluids in the basal turn of cochlea (1^{st}), vestibule (Vest), and ampulla of semicircular canal on the delivery side (L) were smaller than that on the contralateral side (R) 3 h after administration, which progressed one day later (1 d) and remained stable in 2 w. **A:** Cochlear MRI at 3 h after administration; **B:** Vestibular MRI at 3 h post-administration; **C:** Cochlear MRI on 1 d after administration; **D:** Vestibular MRI on 1 d post-administration; **E:** Cochlear MRI on 2 w after administration; **F:** Vestibular MRI on 2 w post-administration. 2^{nd}: second turn of cochlea; **L**: Left; **R**: Right. Scale

bar=1.0 mm

signal in the endolymphatic spaces of the cochlear hook region and vestibule including ampulla became visibly significantly brighter than that in the contralateral side (Figure 6) [15]. Similar morphology was visualized in both inner ears of rats receiving middle ear administration of tetra-branched anti-TNF-α-peptide-conjugated CAN-γ-Fe_2O_3 NPs at 50% peptide ratio. However, no cell population or structure specific distribution of CAN-γ-Fe_2O_3 NPs conjugated to tetra-branched anti-TNF-α peptide was observed (Figure 7).

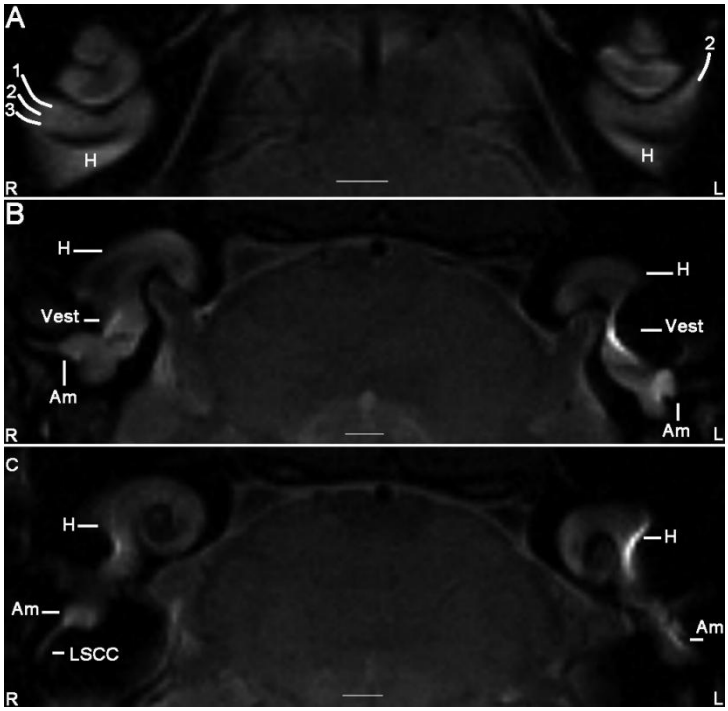

Figure 6: Signal changes in rat inner ear on 1 d post-middle ear administration of tetra-branched anti-TNF-α-peptide-conjugated CAN-γ-Fe_2O_3 NPs at 10% peptide ratio shown by MRI. The narrow strips in the cochlear basal turn and hook region of the delivery ear (L) suggest the scala media **(2)** while the perilymph signal in the scala vestibuli **(1)** and scala tympani **(3)** were wiped out due to distribution of tetra-branched anti-TNF-α-peptide-conjugated CAN-γ-Fe_2O_3 NPs **(A)**. The remnant endolymph signal in vestibule (Vest) **(B)**, ampulla (Am) of the semicircular canal, and hook region of cochlea (H) **(C)** became bright. **LSCC:** Lateral semicircular canal; **L**: Left; **R**: Right. Scale bar=1.0 mm

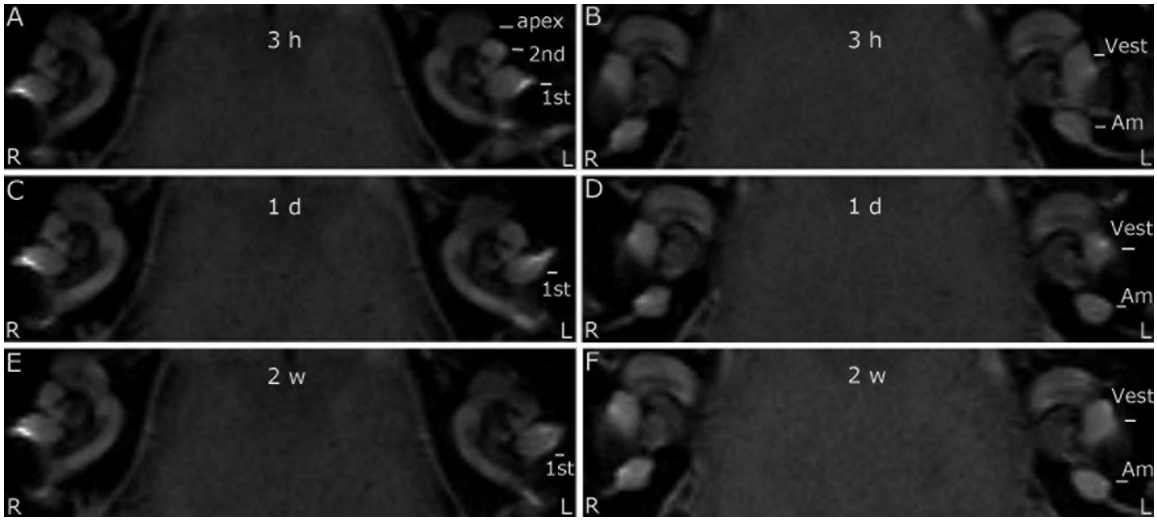

Figure 7: Insignificant rat inner ear entry of tetra-branched anti-TNF-α-peptide-conjugated CAN-γ-Fe_2O_3 NPs at 50% peptide ratio shown by MRI. The cochlea and vestibule (Vest) showed symmetric images on both the delivery (L) and contralateral (R) sides at the time points of 3 h **(A, B)**, 1 d **(C, D)** and 2 w **(E, F)**. Am: ampulla of the semicircular canal; 1^{st}: basal turn of cochlea; 2^{nd}: second turn of cochlea; **L**: Left; **R**: Right. Scale bar=1.0 mm

Inner ear distributions of tetra-branched anti-TNF-α-peptide-conjugated CAN-γ-Fe_2O_3 NPs were histologically detected using

Prussian blue staining (Figure 8 and 9). In accordance with the MRI results, CAN-γ-Fe_2O_3 NPs conjugated to tetra-branched anti-TNF-α peptide at 50% peptide ratio did not sufficiently enter the inner ear (Figure 9).

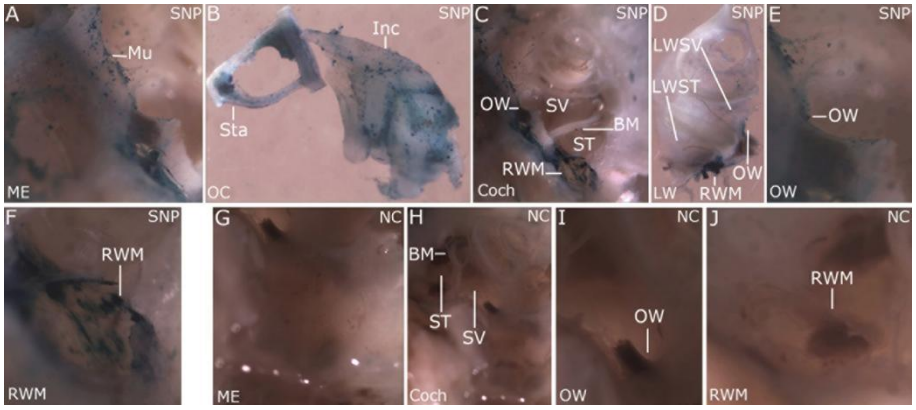

Figure 8: Middle and inner ear distributions of tetra-branched anti-TNF-α-peptide-conjugated CAN-γ-Fe_2O_3 NPs at 10% peptide ratio post-transtympanic injection shown by Prussian blue staining and light microscopy. **BM**: Basilar membrane of cochlea; **Coch**: Cochlea; **Inc**: Incus; **LWST**: Lateral wall of the scala tympany; **LWSV**: Lateral wall of the scala vestibuli; **ME**: Middle ear; **Mu**: Mucosa; **NC**: Negative control; **OC**: Ossicular chain; **OW**: Oval window; **RWM**: Round window membrane; **SNP**: Superparamagnetic nanoparticle; **ST**: Scala tympani; **Sta**: Stapes; **SV**: Scala vestibuli

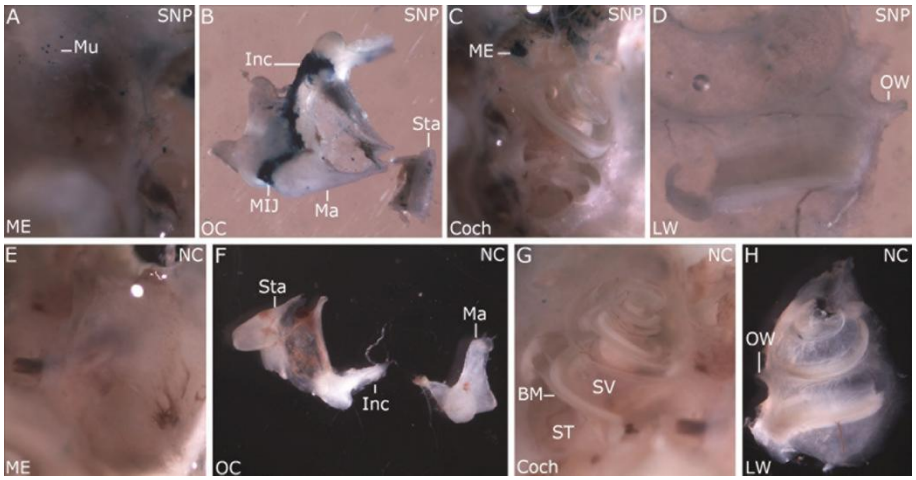

Figure 9: Insufficient inner ear entering of tetra-branched anti-TNF-α-peptide-conjugated CAN-γ-Fe_2O_3 NPs at 50% peptide ratio post-transtympanic injection shown by Prussian blue staining and light microscopy. **BM**: Basilar membrane of cochlea; **Coch**: Cochlea; **Inc**: Incus; **Ma**: Malleus; **ME**: Middle ear; **MIJ**: Malleus-incus joint; **Mu**: Mucosa; **NC**: Negative control; **OC**: Ossicular chain; **OW**: Oval window; **RWM**: Round window membrane; **SNP**: Superparamagnetic nanoparticle; **ST**: Scala tympani; **Sta**: Stapes; **SV**: Scala vestibuli

Discussion

This study shown that in HUVECs stimulated by TNF-α, the tetra-branched anti-TNF-α peptide significantly inhibited apoptosis in comparison to the linear anti-TNF-α peptide. Based on the findings, CAN-γ-Fe2O3 NPs coupled with tetra-branched anti-TNF-α peptide at a peptide ratio of 10% (but not 50%) successfully entered the inner ear and were mostly distributed in the perilymphatic areas after being given to the rats' middle ear. The findings confirmed what was previously stated [13]: the newly found CAN-γ-Fe2O3 NPs were capable of transporting the distinctive tetra-branched anti-TNF-α peptide from the middle ear to the inner ear. The tetra-branched anti-TNF-α peptide was able to be detected by MRI after conjugating with CAN-γ-Fe2O3 NPs, which might make it a valuable theranostics agent. The peptides may be able to independently traverse the middle-inner ear barriers and get in the inner ear. Figure 5 shows that the tetra-branched anti-TNF-α peptide nearly completely suppressed the inhibitory impact on HUVECs produced by TNF-α in the in vitro study, but the linear anti-TNF-α peptide diminished less than half of the effect. The branched anti-TNF-α peptide demonstrated that human melanoma cells expressing TNF-α receptors could not bind to TNF-α. Cells have never been proven to be protected against the activation of the TNF-α receptor signaling pathway by the tetra-branched anti-TNF-α peptide previously [10]. Almost similar binding kinetics were observed between human TNF-α and TNF-α-specific peptides synthesized in linear and tetrameric forms [10]. Compared to the linear anti-TNF-α peptide, the tetra-branched one may have been more efficient in suppressing TNF-α-induced apoptosis in HUVECs. The binding of the TNF-α-specific peptide to human TNF-α at various sites keeps the affinity to the TNF-α-receptor intact. The tetra-branched anti-TNF-α peptide is more likely to block the receptor than the linear one, which has a smaller spatial volume because of its three-

dimensional conformation.

location on the human TNF-α receptor where the receptor binds. This study found evidence that the new tetra-branched anti-TNF-α peptide might be used to treat disorders linked to the activation of the TNF-α receptor in clinical settings. The dynamics of the new peptides in the inner ear may be better understood by in vivo monitoring of the tetra-branched anti-TNF-α peptide, which is an important concern for therapeutic research quality control. An appropriate tool for tracking the kinetics of treatments in the inner ear, particularly in the perilymph and endolymph, the key buffering systems of the inner ear, the new CAN-γ-Fe2O3 NP are a powerful T2-contrast agent ascribed by superparamagnetic effect [13]. The results of the current study shown that tetra-branched anti-TNF-α peptide reached its maximum concentration in the inner ear 1 day after delivery to the middle ear and stayed there for a minimum of 2 weeks. It was shown that the kinetics of pristine CAN-γ-Fe2O3 NPs were much faster than those of CAN-γ-Fe2O3 NPs conjugated to tetra-branched anti-TNF-α peptide at a peptide ratio of 10% [13]. It was shown that the kinetics of the tetra-branched anti-TNF-α peptide, not plain CAN-γ-Fe2O3 NPs, was reflected by the dynamic dispersion of these nanoparticles in the inner ear of rats.

Conclusion

Ultimately, the results showed that compared to the linear anti-TNF-α peptide, the tetra-branched one was more effective in reducing apoptosis in TNF-α driven HUVECs. After being administered to the middle ear of rats, CAN-γ-Fe2O3 NPs conjugated to tetra-branched anti-TNF-α peptide at a peptide ratio of 10% were shown to successfully penetrate the inner ear and disperse in the perilymphatic regions. However, this efficiency was not achieved at proportions of 50%. The research indicated that the new CAN-γ-Fe2O3 nanoparticles can transport the tetra-branched anti-TNF-α peptide from the middle ear to the inner ear, as previously described. The tetra-branched anti-TNF-α peptide was given the ability to be seen by magnetic resonance imaging (MRI) by being coordinatedly conjugated onto CAN-γ-Fe2O3 nanoparticles. This makes it a candidate for use as a theranostics agent. The new peptide and CAN-γ-Fe2O3 NPs were both greatly expanded in the current investigation.

References

1. In a study conducted by Fujioka et al. (2006), the expression of proinflammatory cytokines was examined in noise-induced injury to the cochlea. Published in the Journal of Neuroscience Research, volume 83, pages 575–578. 2. Van der Linden, Thorne, and Vlajkovic (2016) Acute and chronic noise-induced cochlear inflammation in mice: a characterization study. The article is published in Histochem Cell Biol 146, pages 219-30.III. Ren J, Li H, and Lu Y (1998) [Tumor necrosis factor and interleukin 6 measurements in serum of individuals with acute sensorineural hearing loss]. No. 12: 311-3 (Lin Chuang Er Bi Yan Hou Ke Za Zhi). 4. TNF-alpha, IL-10, and IL-12 blood levels in idiopathic spontaneous sensorineural hearing loss (SHL) were studied by Demirhan et al. (2013). Volume 123, Issue 7, Pages 1778–1781, Laryngoscope. 5. Distler GI (1972) Using decorating techniques to investigate the attributes of the solid-state structure. University of the Soviet Union Journal of Physics 36: 1846. The role of unconjugated bilirubin in inflammatory signaling pathways that activate astrocytes was discussed in a 2006 study by Fernandes et al. Published in the Journal of Neurochemistry, volume 96, pages 1667–1679. 7. In a 2006 study, Van Wijk et al. found that autoimmunize neurosensory hearing loss was improved by local perfusion of the tumor necrosis factor alpha blocker infliximab to the inner ear. Article published in the journal Audiol Neurootol on page 357 in the 11th edition.
In 2014, Derebery et al. conducted an open-label trial to see if intratympanic golimumab treatment was safe and effective for individuals with autoimmune inner ear disease. Presented in the journal Otol Neurotol, volume 35, pages 1515–1521. By improving cochlear blood flow in vivo, etanercept-induced TNF-alpha suppression protects against noise-induced hearing loss (Arpornchayanon W, Canis M, Ihler F, Settevendemie C, Strieth S, 2013). The International Journal of Audiology, volume 52, pages 545-552. 10. In a study conducted by Brunetti et al. (2014), it was shown that a unique peptide that was chosen from a phage library may prevent human TNF-alpha from binding to its receptors. In a study published in Molecules, the authors Zou et al. (2010) used 4.7T MRI to assess the differential transit of gadolinium across the inner ear barriers of mice. Histology 259: 36-43. 12. Surface doping with cerium atoms controls the aggregation of hydrophilic maghemite (gamma-Fe2O3) nanoparticles (Haviv AH, Greneche JM, Lellouche JP, 2010). The article "Efficient penetration of ceric ammonium nitrate oxidant-stabilized gamma-maghemite nano-particles into the inner ear of rats as demonstrated by MRI" was published in the Journal of the American Chemical Society and can be found on pages 12519–12521. The authors of the study were Zou et al. (2016). J Biomed Mater Res B Appl Biomater 105: 1883-91. 14. Zou et al. (2011) Effect of ultra-small-volume Gd-DOTA injection on the inner ear of rats: a dynamic enhancement study. 15. MRI manifestation of new superparamagnetic iron oxide nanoparticles in the inner ear of rats as reported in the ORL J Otorhinolaryngol Relat Spec 73: 275-81. (Zou et al., 2010). Published in Nanomedicine (Lond) 5: 739–754.